Applied Physics Letters

Out-of-plane electromechanical coupling in transition metal dichalcogenides

Cite as: Appl. Phys. Lett. **116**, 053101 (2020); https://doi.org/10.1063/1.5134091
Submitted: 29 October 2019 . Accepted: 14 January 2020 . Published Online: 03 February 2020

Christopher J. Brennan, Kalhan Koul, Nanshu Lu, and Edward T. Yu

Applied Physics Letters ARTICLE scitation.org/journal/apl

Out-of-plane electromechanical coupling in transition metal dichalcogenides

Cite as: Appl. Phys. Lett. **116**, 053101 (2020); doi: 10.1063/1.5134091
Submitted: 29 October 2019 · Accepted: 14 January 2020 ·
Published Online: 3 February 2020

Christopher J. Brennan,[1] Kalhan Koul,[1] Nanshu Lu,[1,2,3,4,a)] and Edward T. Yu[1,4,a)]

AFFILIATIONS

[1]Department of Electrical and Computer Engineering, University of Texas at Austin, Austin, Texas 78712, USA
[2]Center for Mechanics of Solids, Structures and Materials, Department of Aerospace Engineering and Engineering Mechanics, University of Texas at Austin, Austin, Texas 78712, USA
[3]Department of Biomedical Engineering, University of Texas at Austin, Austin, Texas 78712, USA
[4]Texas Materials Institute, University of Texas at Austin, Austin, Texas 78712, USA

[a)]**Authors to whom correspondence should be addressed:** nanshulu@utexas.edu. **Tel.:** 512-471-4208 and ety@ece.utexas.edu. **Tel.:** 512-232-5167

ABSTRACT

Monolayer transition metal dichalcogenides (TMDs) are intrinsically piezoelectric within the plane of their atoms, but out-of-plane piezoelectric response should not occur due to the symmetry of the crystal structure. Recently, however, MoS_2 was shown to exhibit out-of-plane electromechanical coupling consistent with the flexoelectric effect. In this study, $MoSe_2$, WS_2, and WSe_2 are investigated to determine the existence and strength of out-of-plane electromechanical coupling in other monolayer TMD semiconductor materials. Piezoresponse force microscopy measurements show that monolayer MoS_2, $MoSe_2$, WS_2, and WSe_2 all exhibit out-of-plane electromechanical response. The relative magnitudes of their out-of-plane electromechanical couplings are calculated and compared with one another and to predictions made from a simple model of flexoelectricity. This simple model correctly predicts the magnitude of out-of-plane electromechanical response in these materials, and the measured values provide useful guidance for both more detailed understanding of flexoelectric response in monolayer TMDs, and assessment of their consequences in devices incorporating these materials.

Transition metal dichalcogenides (TMDs) are a class of layered materials which, because adjacent layers are typically bound by van der Waals interactions, are amenable to separation into atomically thin monolayer or few-layer films—so-called two-dimensional materials. In comparison to graphene, which is typically metallic or semimetallic, atomically thin TMDs have nonzero energy bandgaps and are therefore particularly attractive for electronic and optoelectronic device applications. Their semiconducting nature and atomic thinness make TMDs particularly interesting for use in flexible electronics because of the ability to control their electronic properties via mechanical strain, and their very low bending stiffness, which decreases greatly with decreasing thickness. Additionally, TMDs have been shown to withstand strains up to 11% experimentally[1] and 28% theoretically[2] making them resistant to mechanical failure.[3] As such, TMDs offer promise for use in flexible electronics,[4] where they would be expected to endure frequent, and often substantial, stress and strain. The use of TMDs in flexible electronics is, however, predicated on fully understanding how their electronic properties will vary with strain.

In addition, strain can be harnessed to intentionally control the electronic properties of TMDs via strain engineering. Such examples include using strain to alter a material's bandgap to change its optical properties,[5] to influence the carrier mobility to improve electrical performance,[6] to alter its conductivity for use in strain sensing applications,[7] or to create electromechanical energy harvesters by taking advantage of the repeated strain environment that can be experienced by TMDs.[8] A key aspect of the relationship between strain and electronic properties is electromechanical coupling, in which dielectric polarization and internal electric fields are created within a material due to an applied strain, or vice versa. More specifically, piezoelectricity and flexoelectricity are properties where an electric field is created from an applied uniform strain or strain gradient, respectively. Monolayer TMDs inherently possess piezoelectricity within the plane of their atoms due to a lack of inversion symmetry, which has been experimentally measured,[9,10] but do not possess out-of-plane piezoelectricity.[11] In addition, monolayer MoS_2 was recently shown experimentally to exhibit out-of-plane electromechanical coupling, which

has been attributed to flexoelectricity.[12] Similar findings have also been shown for few-layer $MoTe_2$ but have been attributed to a corrugation effect due to a rough substrate.[13]

In this study, the out-of-plane electromechanical coupling properties of three different semiconducting TMDs—$MoSe_2$, WS_2, and WSe_2—are measured and compared to measurements of electromechanical coupling in MoS_2. The measured values are of the same order-of-magnitude for all four materials studied, and demonstrate that out-of-plane flexoelectricity is exhibited across a variety of 2D TMDs materials. Moreover, the order-of-magnitude of the measured values agrees well with predictions made from a simple model of flexoelectricity proposed by Kogan.[14]

All samples are created via mechanical exfoliation from bulk crystals using a blue polyethylene cleanroom tape. The TMDs are first transferred from the tape to a Polydimethylsiloxane (PDMS) stamp, and then from the PDMS stamp to a gold-coated silicon substrate while heating the sample at 70 °C on a hot plate for 5 min. Slowly peeling the PDMS away transfers the TMD onto the gold. It is found that the TMDs transfer more readily onto the gold substrate using the intermediate PDMS stamp instead of transferring directly from the tape to the gold-coated substrate. Monolayer regions of TMD materials are identified and then characterized using piezoresponse force microscopy (PFM) with experimental details given in the supplementary material, closely following previous work.[12] Briefly, a sinusoidal alternating voltage is applied between a conductive atomic force microscopy (AFM) probe and the gold substrate to create an electric field across the TMD material. If the TMD is electromechanically active, it will expand and contract in response to the applied electric field, and the resulting vertical deformation is measured by the deflection of the AFM cantilever, as shown in Fig. 1. As described in detail elsewhere,[12] the sample preparation and measurement process employed here are able to distinguish out-of-plane electromechanical response from in-plane piezoelectricity and avoid spurious contributions to PFM response from potential surface contamination or other artifacts.

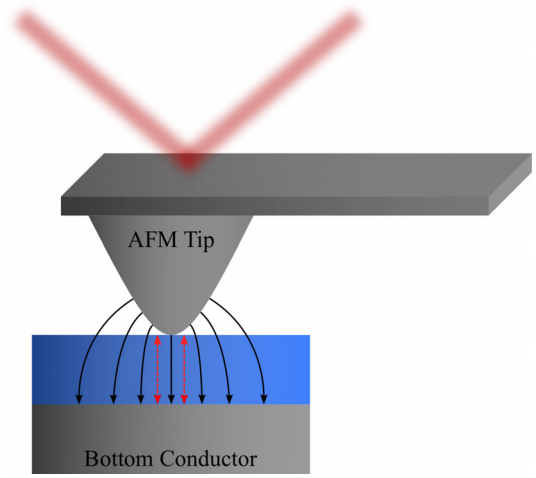

FIG. 1. A schematic illustration of an AFM tip as used in a PFM measurement. The AFM tip is made of a conductive material, cobalt–chromium here, to be able to apply an electric field (black arrows) across the TMD (blue) materials. The electric field causes the TMD to expand and contract vertically (red arrows), which is detected by the AFM cantilever moving with the TMD, and measured by a laser reflecting off the top of the cantilever and hitting a position sensitive photodiode.

Optical images of the $MoSe_2$, WSe_2, and WS_2 layers characterized by PFM are shown in Figs. 2(a), 2(d), and 2(g), respectively. To the right of each optical image is a tapping-mode AFM image taken within the red box superimposed on the adjacent optical image. Raman spectra are measured for the $MoSe_2$ [Fig. 2(c)] and WSe_2 [Fig. 2(f)] layers for both monolayer and multilayer regions to confirm the presence of the monolayer material. The selenium-based TMDs have a distinctive Raman peak that is present in few-layered samples but vanishes in monolayer and bulk material. In $MoSe_2$, this is the B_{2g} mode near 355 cm^{-1}, which vanishes in the monolayer limit [Fig. 2(c)].[15] The large peak near 245 cm^{-1} is the A' peak (A_{1g} in multilayer $MoSe_2$). In the WSe_2 sample, the distinctive multilayer Raman peak is at ~310 cm^{-1} and has been shown to vanish in monolayer material[15,16] [Fig. 2(f)]. The origin of this peak is most likely an interlayer shear mode. For WS_2, photoluminescence (PL) is more easily used to confirm the presence of monolayer material. Monolayer WS_2 is a direct bandgap semiconductor, while multilayer WS_2 is indirect; thus, monolayer WS_2 will luminesce more strongly than multilayer material. This is seen in the PL measurement in Fig. 2(i), where the displayed multilayer signal has been multiplied by a factor of two. A second peak also appears in PL from multilayer but not monolayer WS_2, which originates from the indirect gap, providing another distinguishing feature of monolayer WS_2.[17]

Results of PFM measurements performed on the samples shown in Fig. 2 are presented in Fig. 3. An AFM height image is simultaneously captured during the PFM measurements [Figs. 3(a), 3(d), and 3(g)] and shown along with the corresponding PFM amplitude and phase channel images. A drive voltage of amplitude 7 V and frequency 60 kHz is applied between the tip and gold substrate induces contrast within the PFM amplitude and phase channels for the $MoSe_2$ [Figs. 3(b) and 3(c)], WSe_2 [Figs. 3(e) and 3(f)], and WS_2 [Figs. 3(h) and 3(i)] regions compared to the underlying gold substrate. The contrast observed indicates that there is out-of-plane electromechanical coupling arising from the TMD material.[12] Without applying the drive voltage, the contrast vanishes, indicating that scanning artifacts likely do not contribute to the signal (supplementary material Figs. 1–3). These effects, along with electrostatic effects which are not seen here, are discussed at length in our previous work.[12] Furthermore, the near-identical topography images before and after applying the drive voltage show that the voltage did not affect the AFM tip or sample.

A background subtraction method[12] is used to calculate the effective out-of-plane sample response and a corresponding effective piezoelectric coefficient, d_{33}^{eff}, where the background is taken to be the signal measured on the gold substrate. Multiple measurements of monolayer regions are taken for each TMD, and the results are summarized in Table I. The measurement results shown in Table I for MoS_2 are from a separate sample than presented in the previous work by Brennan *et al.*,[12] and corresponding AFM and PFM images are shown in the supplementary material, Fig. 4. The values measured from the present MoS_2 sample closely match the previously reported results. Calculated values of the in-plane piezoelectric coefficient[11] d_{11} for each TMD material are also shown for a comparison. These calculated in-plane values are the same order-of-magnitude as the out-of-plane values

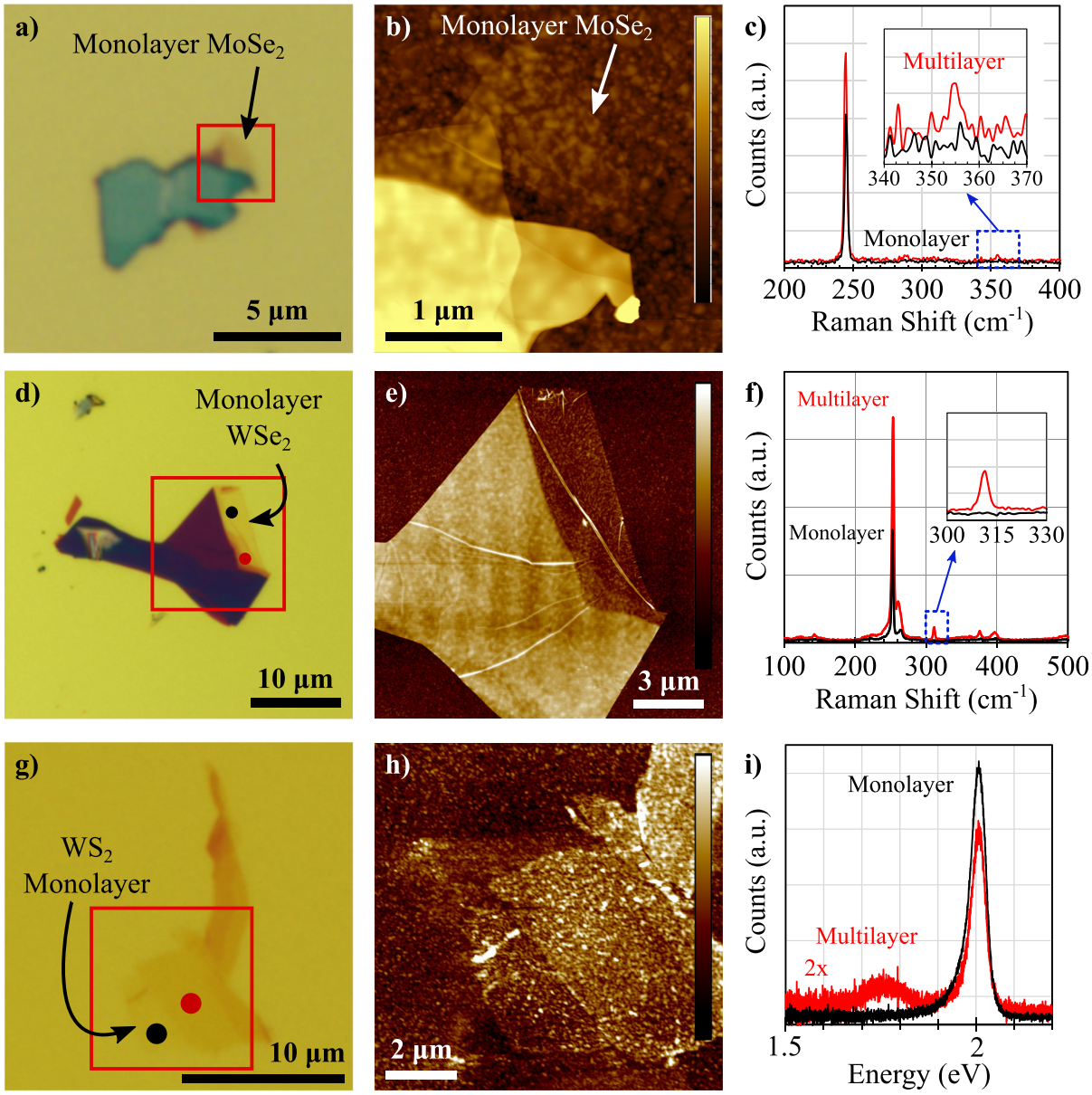

FIG. 2. Characterization of $MoSe_2$ (a)–(c), WSe_2 (d)–(f), and WS_2 (g)–(i) used in PFM measurements. For each material, an optical microscope image (a), (d), (g), tapping-mode AFM image (b), (e), (h), and Raman (c) and (f) or photoluminescence (i) measurement are shown. The red boxes in the optical images show the locations of the tapping mode images. The color bars in the tapping-mode AFM images correspond to 0 nm–30 nm in (b), 0 nm–26.6 nm for (e), and 0 nm–9.5 nm in (h). For $MoSe_2$ (c), the Raman spectra show the absence of the multilayer peak around 355 cm^{-1} in the monolayer region. The spectrum shown for multilayer $MoSe_2$ was taken from a separate sample for comparison. In the WSe_2 Raman spectrum (f), the absence of the multilayer peak at 310 cm^{-1} confirms that monolayer material is present. For WS_2 (i), photoluminescence confirms the presence of monolayer material via the stronger signal compared to a thicker region, and the absence of the indirect peak. The black and red dots in (d) and (g) indicate the locations from which monolayer and multilayer measurements shown in (f) and (i), respectively, were obtained.

measured here, indicating that the effects measured here are sufficiently strong that their consequence for strain engineering of electronic and optical properties of atomically thin TMD structures may be comparable to those of conventional piezoelectric behavior.

The measured value for d_{33}^{eff} can be converted to a measured effective flexoelectric response, μ_{eff}^{*}, given by[12]

$$\mu_{eff}^{*} \approx \frac{d_{33}^{eff} \cdot Y_{2D}}{2}. \quad (1)$$

This equation originates from the definition of the flexoelectric coefficient, analysis to determine the dominant flexoelectric tensor components which for out-of-plane response are expected to be μ_{39}^{*}

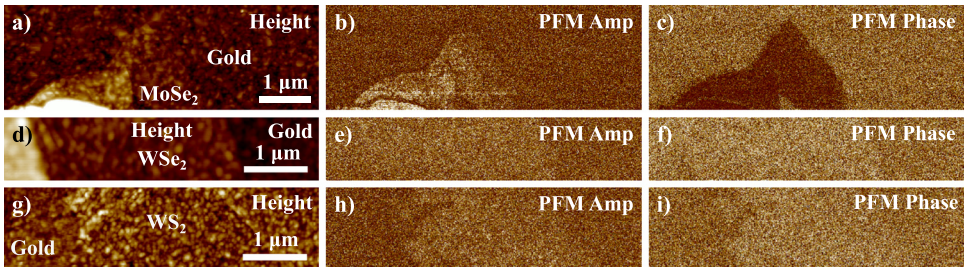

FIG. 3. PFM measurements of $MoSe_2$ (a)–(c), WSe_2 (d)–(f), and WS_2 (g)–(i). For each sample, a contact-mode height image (a), (d), and (g), PFM amplitude image (b), (e), and (h), and PFM phase image (e), (f), and (i) are obtained simultaneously from the same location. The existence of contrast in the PFM amplitude and phase images is indicative of the presence of out-of-plane electromechanical coupling.

and μ^*_{48}, and estimates of the electric field distribution across the TMD material.[12] In Eq. (2), the 2D Young's modulus, Y_{2D}, has units of Newtons per meter and is used here because it is readily calculated from elastic stiffness tensors provided in the literature,[11,18]

$$Y_{2D} = \frac{C_{11}^2 - C_{12}^2}{C_{11}}, \tag{2}$$

where C_{ij} is the elastic stiffness tensor of the corresponding monolayer TMD. The 2D Young's modulus is used because of the absence, or scarcity of, measured Young's modulus values for the TMDs other than MoS_2. Instead of using measured values from different references whose methods may vary, Y_{2D} is used because it is readily calculated, and sometimes given,[18] for all TMDs from data provided from a single Ref. 11 so that more accurate comparisons can be made among the different TMD materials. Also, given in Table I are relevant parameters associated with the TMDs that are used in conjunction with a simple flexoelectric model[14,19] to estimate the expected flexoelectric response.[14,19,20] The basic parameters included are lattice constant,[11] a_0, dielectric susceptibility,[21] χ, and the 2D Young's modulus calculated from density functional theory (DFT) estimates of the elastic stiffness tensor of the TMDs,[11,18] Y_{2D}.

The simple model used to obtain an order-of-magnitude estimate of the flexoelectric response of a material was first developed by Kogan, and yields and estimated value for the flexoelectric coefficient, μ_{est}, are given by[14,19,20]

$$\mu_{est} \approx \frac{q\chi}{4\pi\epsilon_0 a_0}. \tag{3}$$

In this model, flexoelectric response originates from point charges separated by a distance a_0 experiencing a strain gradient $1/a_0$. The dependence of the overall energy density of the material on this perturbation can be assigned to the flexoelectric term in the free-energy expansion of the material.[19] As can be seen in Table I, the resulting values of μ_{est} are somewhat higher than, but generally of the same order-of-magnitude as, the values of μ^*_{eff} obtained experimentally. Both values are approximately one order-of-magnitude lower than theoretical estimates of ferroelectric materials, which is expected to be the lower value of the TMDs relative permittivities.[22] However, the range of measured values is substantially greater than that of the simple theoretical estimates, suggesting that factors other than those accounted for in Kogan's model contribute substantially to flexoelectric response in monolayer TMD materials. Notably, the value measured for $MoSe_2$ is roughly twice as large as the other TMDs, the origin of which is still under investigation.

In summary, monolayer $MoSe_2$, WSe_2, and WS_2 have been shown experimentally to exhibit out-of-plane electromechanical coupling comparable to that demonstrated previously in monolayer MoS_2. PFM measurements on all materials studied are consistent with the observation of out-of-plane flexoelectric response, and the effective flexoelectric coefficients deduced from these measurements are of the same order-of-magnitude as those predicted using a simple model for flexoelectricity. The availability of measured values for μ^*_{eff} in MoS_2, $MoSe_2$, WS_2, and WSe_2 is expected to provide valuable guidance for both more detailed understanding of flexoelectric response in monolayer TMDs, and assessment of its consequences in devices incorporating these materials.

TABLE I. A summary of the data used to compare the electromechanical responses of the different TMDs. The general parameters considered are the lattice constant, a_0, the dielectric susceptibility, χ, 2D Young's modulus, Y_{2D}, and calculated in-plane piezoelectric coefficient d_{11}. The estimated flexoelectric response, μ_{est}, is shown with the measured out-of-plane effective piezoelectric response, d^{eff}_{33}, and effective flexoelectric response, μ^*_{eff} obtained based on d^{eff}_{33}.

TMD	a_0[11] (Å)	χ[21,a]	Y_{2D}[11] (N/m)	d_{11}[11] (pm/V)	μ_{est} (nC/m)	d^{eff}_{33} (pm/V)	μ^*_{eff} (nC/m)
MoS_2	3.19	3.26	137.9	3.73	0.130	0.94 ± 0.03	0.065
$MoSe_2$	3.32	3.74	113.8	4.72	0.144	1.82[b]	0.103
WS_2	3.19	3.13	150.7	2.19	0.125	0.71 ± 0.19	0.053
WSe_2	3.32	3.63	123.1	2.79	0.139	0.43 ± 0.11	0.026

[a]The dielectric susceptibility is taken to be $\epsilon^{\perp}_{mac} - 1$ from Ref. 21.
[b]No standard deviation was given because the value is from a single measurement.

See the supplementary material for the experimental PFM details, PFM of $MoSe_2$ with and without the drive voltage applied, PFM of WS_2 with and without the drive voltage applied, PFM of WSe_2 with and without the drive voltage applied, and PFM of new MoS_2 sample for comparison with previous work.

AUTHOR'S CONTRIBUTIONS

C.J.B. performed the sample fabrication, AFM, PFM, Raman, photoluminescence, and data analysis for $MoSe_2$, WSe_2, and MoS_2. K.K. performed the sample fabrication, AFM, PFM, Raman, photoluminescence, and data analysis for WS_2. N.L. and E.T.Y. assisted in the project design and supervised the research. C.J.B., N.L., and E.T.Y. wrote the manuscript.

This work was supported by the NSF CMMI Award under Grant No. 1351875 and NSF DMR Award under Grant Nos. DMR-1311866 and DMR-1905287. We acknowledge the use of Texas Nanofabrication Facilities supported by the NSF NNCI Award under No. 1542159. E.T.Y. acknowledges the Judson S. Swearingen Regents Chair in Engineering at the University of Texas at Austin. C.J.B. acknowledges Dr. Brooks Carlton Fowler Endowed Presidential Graduate Fellowship in Electrical and Computer Engineering and the Temple Foundation Graduate Microelectronic and Computer Development Fellowship in Engineering of UT-Austin. Thanks to Professor Sanjay K. Banerjee's research group for bulk $MoSe_2$, Professor Emanuel Tutuc's research group for bulk WS_2, and Professor Ananth Dodabalapur's research group for bulk WSe_2.

REFERENCES

[1]S. Bertolazzi, J. Brivio, and A. Kis, "Stretching and breaking of ultrathin MoS_2," ACS Nano **5**(12), 9703–9709 (2011).
[2]T. Li, "Ideal strength and phonon instability in single-layer," Phys. Rev. B **85**(23), 235407 (2012).
[3]D. Akinwande, C. J. Brennan, J. S. Bunch, P. Egberts, J. R. Felts, H. Gao, R. Huang, J.-S. Kim, T. Li, Y. Li *et al.*, "A review on mechanics and mechanical properties of 2D materials—graphene and beyond," Extreme Mech. Lett. **13**, 42–77 (2017).
[4]D. Akinwande, N. Petrone, and J. Hone, "Two-dimensional flexible nanoelectronics," Nat Commun **5**, 5678 (2014).
[5]D. Lloyd, X. Liu, J. W. Christopher, L. Cantley, A. Wadehra, B. L. Kim, B. B. Goldberg, A. K. Swan, and J. S. Bunch, "Band gap engineering with ultralarge biaxial strains in suspended monolayer MoS_2," Nano Lett. **16**(9), 5836–5841 (2016).
[6]S. Manzeli, D. Ovchinnikov, D. Pasquier, O. V. Yazyev, and A. Kis, "2D transition metal dichalcogenides," Nat. Rev. Mater. **2**(8), 17033 (2017).
[7]S. Manzeli, A. Allain, A. Ghadimi, and A. Kis, "Piezoresistivity and strain-induced band gap tuning in atomically thin MoS_2," Nano Lett. **15**(8), 5330 (2015).
[8]P.-K. Yang and C.-P. Lee, *2D-Layered Nanomaterials for Energy Harvesting and Sensing Applications* (IntechOpen, 2019).
[9]W. Wu, L. Wang, Y. Li, F. Zhang, L. Lin, S. Niu, D. Chenet, X. Zhang, Y. Hao, T. F. Heinz *et al.*, "Piezoelectricity of single-atomic-layer MoS_2 for energy conversion and piezotronics," Nature **514**(7523), 470–474 (2014).
[10]H. Zhu, Y. Wang, J. Xiao, M. Liu, S. Xiong, Z. J. Wong, Z. Ye, Y. Ye, X. Yin, and X. Zhang, "Observation of piezoelectricity in free-standing monolayer MoS_2," Nat. Nanotechnol. **10**(2), 151–155 (2015).
[11]K. A. N. Duerloo, M. T. Ong, and E. J. Reed, "Intrinsic piezoelectricity in two-dimensional materials," J. Phys. Chem. Lett. **3**(19), 2871–2876 (2012).
[12]C. J. Brennan, R. Ghosh, K. Koul, S. K. Banerjee, N. Lu, and E. T. Yu, "Out-of-plane electromechanical response of monolayer molybdenum disulfide measured by piezoresponse force microscopy," Nano Lett. **17**(9), 5464–5471 (2017).
[13]S. Kang, S. Jeon, S. Kim, D. Seol, H. Yang, J. Lee, and Y. Kim, "Tunable out-of-plane piezoelectricity in thin-layered $MoTe_2$ by surface corrugation-mediated flexoelectricity," ACS Appl. Mater. Interfaces **10**, 27424–27431 (2018).
[14]S. M. Kogan, "Piezoelectric effect during inhomogeneous deformation and acoustic scattering of carriers in crystals," Sov. Phys. Solid State **5**(10), 2069–2070 (1964).
[15]P. Tonndorf, R. Schmidt, P. Böttger, X. Zhang, J. Börner, A. Liebig, M. Albrecht, C. Kloc, O. Gordan, D. R. T. Zahn *et al.*, "Photoluminescence emission and Raman response of monolayer MoS_2, $MoSe_2$, and WSe_2," Opt. Express **21**(4), 4908 (2013).
[16]W. Zhao, Z. Ghorannevis, K. K. Amara, J. R. Pang, M. Toh, X. Zhang, C. Kloc, P. H. Tan, and G. Eda, "Lattice dynamics in mono- and few-layer sheets of WS_2 and WSe_2," Nanoscale **5**(20), 9677 (2013).
[17]W. Zhao, Z. Ghorannevis, L. Chu, M. Toh, C. Kloc, P. H. Tan, and G. Eda, "Evolution of electronic structure in atomically thin sheets of WS_2 and WSe_2," ACS Nano **7**(1), 791–797 (2013).
[18]M. M. Alyoruk, Y. Aierken, C. Deniz, F. M. Peeters, and C. Sevik, "Promising piezoelectric performance of single layer transition-metal dichalcogenides and dioxides," The Journal of Physical Chemistry C, **119**(40), 23231–23237 (2015).
[19]P. V. Yudin and a. K. Tagantsev, "Fundamentals of flexoelectricity in solids," Nanotechnology **24**(43), 432001 (2013).
[20]P. Zubko, G. Catalan, and A. K. Tagantsev, "Flexoelectric effect in solids," Annu. Rev. Mater. Res. **43**(1), 387–421 (2013).
[21]A. Ramasubramaniam, "Large excitonic effects in monolayers of molybdenum and tungsten dichalcogenides," Phys. Rev. B **86**(11), 115409 (2012).
[22]B. Wang, Y. Gu, S. Zhang, and L. Chen, "Flexoelectricity in solids: Progress, challenges, and perspectives," Prog. Mater. Sci. **106**, 100570 (2019).

Supporting Information

Out-of-Plane Electromechanical Coupling in Transition Metal Dichalcogenides

Christopher J. Brennan[1], Kalhan Koul[1], Nanshu Lu[1,2,3,4], Edward T. Yu[1,4*].*

[1]Department of Electrical and Computer Engineering, University of Texas at Austin, Austin, (TX), 78712 USA

[2]Center for Mechanics of Solids, Structures and Materials, Department of Aerospace Engineering and Engineering Mechanics, University of Texas at Austin, Austin, (TX), 78712 USA

[3]Department of Biomedical Engineering, University of Texas at Austin, Austin, (TX), 78712 USA

[4]Texas Materials Institute, University of Texas at Austin, Austin, (TX), 78712 USA

* Corresponding authors:

Edward T. Yu, ety@ece.utexas.edu, 512-232-5167, MER 1.206M, 10100 Burnet Rd. Bldg 160, Austin, TX 78758

Nanshu Lu, nanshulu@utexas.edu, 512-471-4208, 210 E. 24th St, Austin, TX 78712

PFM Experimental Details

PFM measurements were done using a Bruker (formerly Veeco) Dimension Icon AFM. Conductive cobalt−chromium AFM cantilevers are used (Bruker MESP-RC-V2) for PFM measurements. Tapping mode AFM images were taken using etched silicon cantilevers (Bruker TESP). A PFM drive frequency of 60 kHz and a drive amplitude of 7 V were used in the presented measurements which had the drive voltage applied. When not applied to the sample, as in right half of the below figures, a 7 V amplitude and 60 kHz frequency signal is still input into the reference channel of PFM lock-in amplifier. A periodically-poled lithium niobite (PPLN) reference sample was previously measured to confirm the detection of oppositely polarized piezoelectric materials. Further details about the PFM experiment can be seen in our previous work "Out-of-Plane Electromechanical Response of Monolayer Molybdenum Disulfide Measured by Piezoresponse Force Microscopy" and it's Supporting Information in Nano Letters (DOI: 10.1021/acs.nanolett.7b02123).

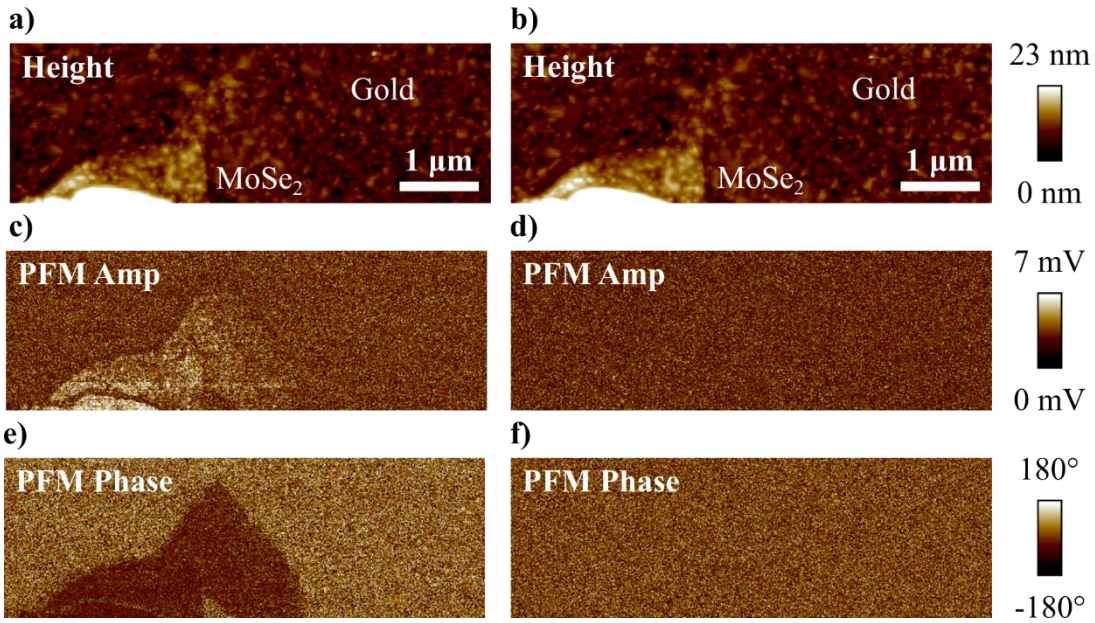

Supplemental Figure 1. PFM measurement of the same $MoSe_2$ sample as in Figure 2 where the height (a,b), PFM amplitude (c,d) and PFM phase (e,f) are shown for with the drive voltage applied (a,c,e) and not applied (b,d,f). Since there is no PFM contrast when the drive voltage is not applied, there are no scanning artifacts.

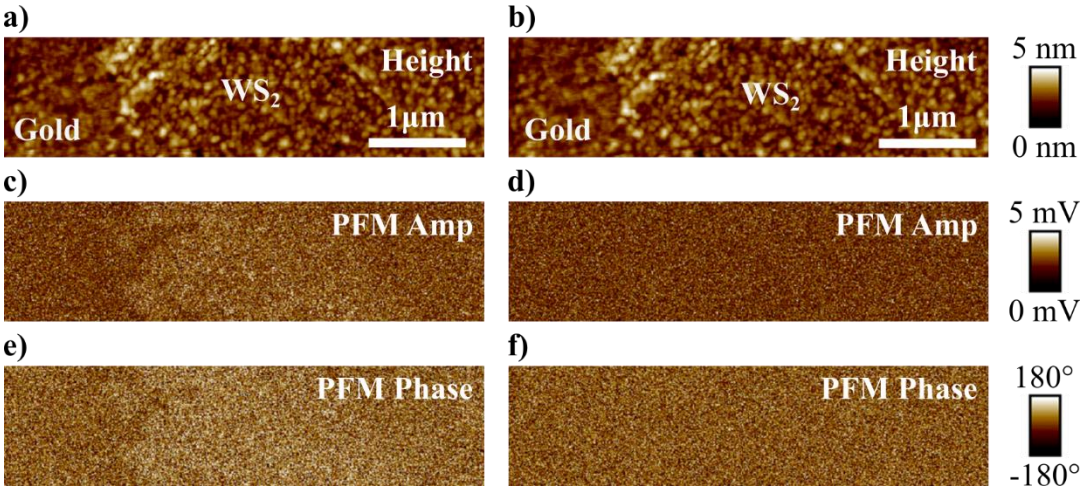

Supplemental Figure 2. PFM measurement of the same WS_2 sample as in Figure 2 where the height (a,b), PFM amplitude (c,d) and PFM phase (e,f) are shown for with the drive voltage applied (a,c,e) and not applied (b,d,f). Since there is no PFM contrast when the drive voltage is not applied, there are no scanning artifacts.

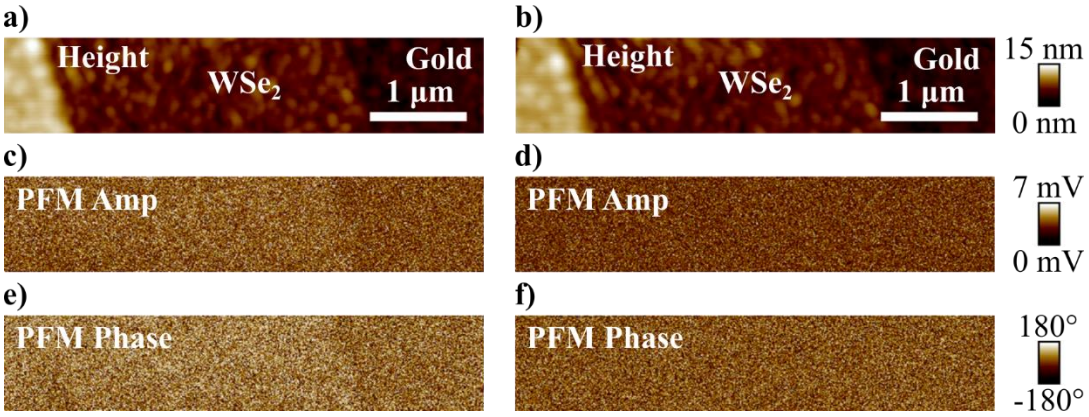

Supplemental Figure 3. PFM measurement of the same WSe_2 sample as in Figure 2 where the height (a,b), PFM amplitude (c,d) and PFM phase (e,f) are shown for with the drive voltage applied (a,c,e) and not applied (b,d,f). Since there is no PFM contrast when the drive voltage is not applied, there are no scanning artifacts.

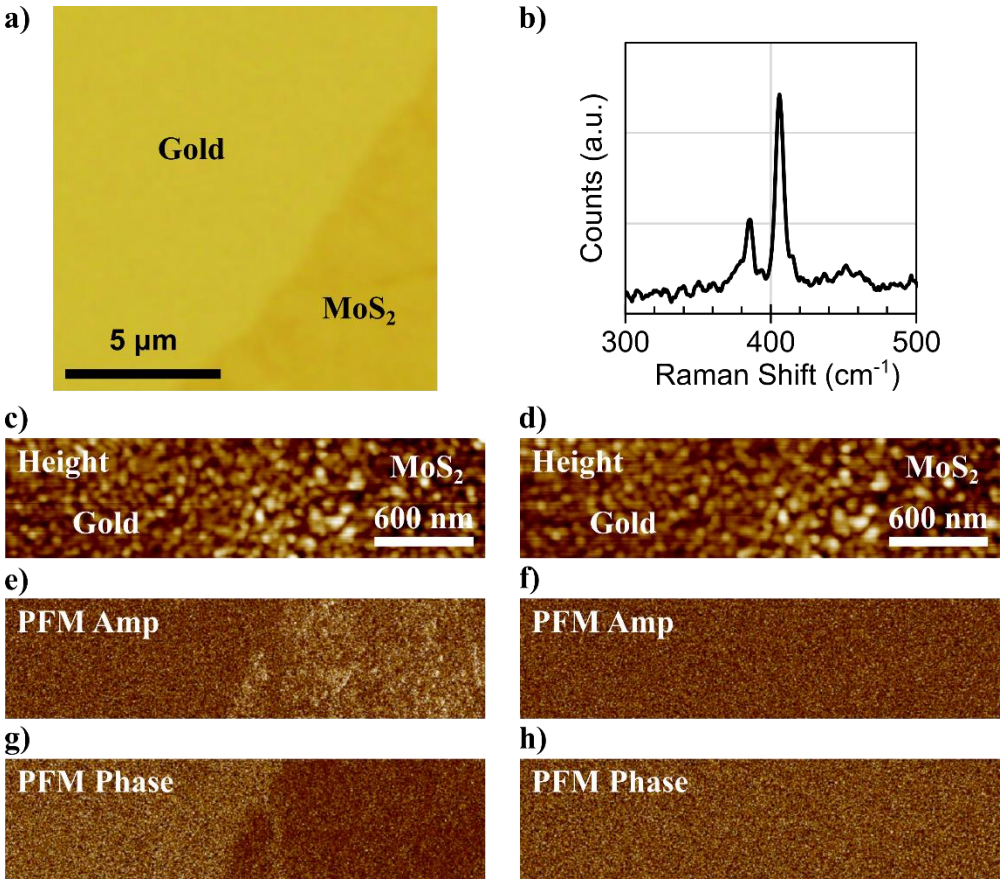

Supplemental Figure 4. (a) Optical microscope image of CVD grown MoS_2 on gold. (b) Raman spectra of the CVD grown MoS_2 in (a) indicates monolayer MoS_2. PFM image on the MoS_2 on gold with the drive voltage on (c,e,g) and with the drive voltage off (d,f,h). The contrast in the PFM amplitude (e) and PFM phase (g) with the drive voltage applied indicates the presence electromechanical coupling. The lack of contrast in the PFM amplitude (f) and PFM phase (h) when the drive voltage not applied indicates no scanning artifacts.